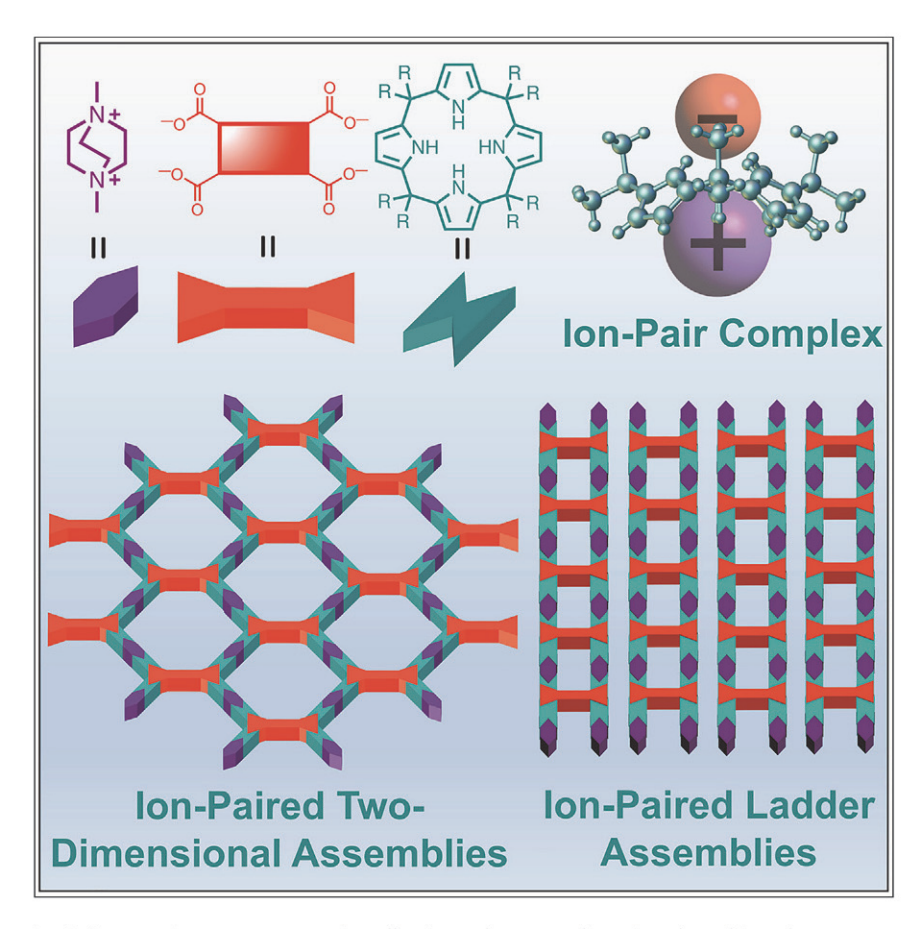
Chem



### Article

## A modular platform for the precise assembly of molecular frameworks composed of ion pairs



Ionic interactions are conventionally viewed as non-directional, making them unappealing for their use in molecular framework materials. Here, we show that calix[4]pyrrole ion-pair receptors orient ion pairs, thereby enabling their predictable assembly into modular, porous frameworks. In some cases, these frameworks were shown to maintain their crystallinity and porosity following solvent removal. This strategy was used to organize tetrathiafulvalene spin-active materials.

Luke P. Skala, Charlotte L. Stern, Laura Bancroft, ..., Jeremy L. Swartz, Michael R. Wasielewski, William R. Dichtel

m-wasielewski@northwestern.edu (M.R.W.) wdichtel@northwestern.edu (W.R.D.)

#### Highlights

Calix[4]pyrrole receptors orient ion pairs into 2D assemblies

Ion-pair assemblies are modular

Some ion-pair assemblies can be activated to provide high-surfacearea materials

Ion-pair assemblies provide molecularly precise solid-state spin arrays



Skala et al., Chem 9, 1208–1220 May 11, 2023 © 2023 Elsevier Inc. https://doi.org/10.1016/j.chempr.2023.01.011







#### Article

# A modular platform for the precise assembly of molecular frameworks composed of ion pairs

Luke P. Skala,<sup>1</sup> Charlotte L. Stern,<sup>1</sup> Laura Bancroft,<sup>1</sup> Casandra M. Moisanu,<sup>1</sup> Chloe Pelkowski,<sup>1</sup> Xavier Aguilar-Enriquez,<sup>1</sup> Jeremy L. Swartz,<sup>1</sup> Michael R. Wasielewski,<sup>1,\*</sup> and William R. Dichtel<sup>1,2,\*</sup>

#### **SUMMARY**

Electrostatic interactions are typically non-directional, which complicates their use for designing ordered molecular frameworks. However, ion-pair receptors, such as calix[4]pyrroles, orient cations in addition to anions with a specific binding geometry in solution and the solid state. This high degree of spatial orientation was leveraged to assemble extended arrays of ion pairs. Calix[4]pyrrole assemblies are highly tunable and modular, as demonstrated in seven examples of 2D layered crystals or 1D ladder polymers characterized by single-crystal X-ray diffraction. Moreover, these assemblies maintain their crystallinity and porosity following the removal of solvent. Single crystals of a 2D framework based on tetrathiafulvalene building blocks were obtained, and the triplet state of these spin-active materials was characterized with transient electron paramagnetic resonance (TREPR) spectroscopy. These results demonstrate that calix[4] pyrrole assemblies are a versatile new class of supramolecular frameworks that hold intriguing possibilities for organizing functional organic subunits into designed solid-state structures.

#### INTRODUCTION

Directional bonding interactions can assemble molecules, <sup>1,2</sup> polymers, <sup>3,4</sup> proteins, <sup>5,6</sup> and nanoparticles<sup>7,8</sup> to provide nano and mesoscale structures that exhibit emergent optical, electrical, and structural properties. <sup>9–14</sup> For molecular building blocks, this approach underlies the design of metal-organic frameworks, <sup>15</sup> covalent-organic frameworks, <sup>16,17</sup> and hydrogen-bonded organic frameworks. <sup>18,19</sup> These frameworks leverage metal coordination, covalent bonds, or hydrogen bonding, all of which exhibit specific directional preferences. By contrast, the electrostatic attractions of ion pairs are not generally used to direct framework structures because they have much more limited directional preferences. Nevertheless, ion pairs would be useful for this purpose, as they are compact, easily introduced into most molecules, and their interaction strengths are tunable by changes in molecular structure or the dielectric constant, pH, or chemical composition of the medium. Developing general strategies to impart directionality to ion pairs will enable entirely new classes of molecular materials.

To explore this possibility, we look to supramolecular receptors that simultaneously bind both anions and cations in a well-defined geometry, <sup>20,21</sup> rather than solely one or the other (e.g., crown ethers, cryptands, and cyclophanes). Calix[4]pyrroles (C4Ps, Figure 1) are one such receptor whose ability to bind ion pairs was recognized in pioneering work by Sessler and coworkers. <sup>22–24</sup> C4P orients ion pairs directionally, both in solution and in the solid state, and recognizes several chemically distinct anions

#### THE BIGGER PICTURE

The precise assembly of molecular building blocks plays a crucial role in designing crystalline, porous organic materials. Typically, the interactions governing assembly, such as covalent, coordination, or hydrogen bonds, point in specific directions that direct the structure of a porous framework material. By contrast, ion-pairing interactions have limited directional preferences and are not typically used for this purpose. Here, we report a new strategy to crystallize porous organic assemblies by using ion-pair receptors, calix[4]pyrroles, to simultaneously bind carboxylate and quaternary ammonium ions. Polyfunctional carboxylate and ammonium ions crystallized either into 2D sheets or supramolecular ladder polymers, with several examples of each type characterized unambiguously using single-crystal X-ray diffraction. This approach offers significant promise as a means of assembling electronically active materials into specific solid-state structures based only on light elements.



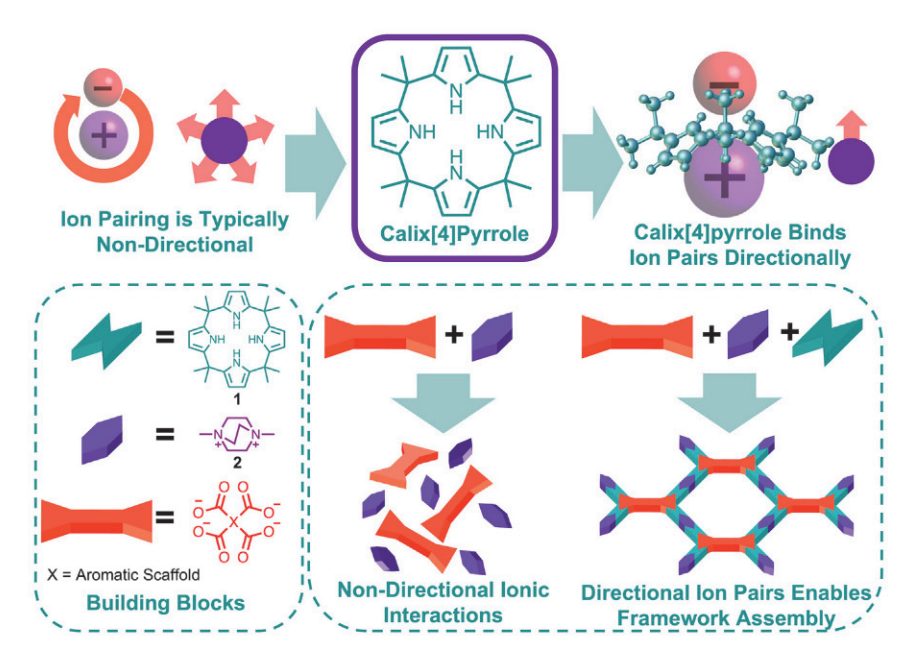


Figure 1. Schematic illustration of the use of ion-pair receptors for framework assembly Schematic depicting how C4Ps enable the directional ion pairing of anions and cations. C4Ps' ability to form directional ion pairs facilitates the assembly of dicationic 2 and carboxylate linkers into porous networks.

and cations. Crystal structures of C4P are known with bound anions including halogens, <sup>22,25–27</sup> carboxylates, <sup>25–28</sup> phenolates, <sup>29</sup> carbonates, <sup>26</sup> N-oxides, <sup>30</sup> nitrates, <sup>25,27</sup> sulfates, <sup>22,25,26</sup> or phosphates. <sup>22,25</sup> The cations include quaternary ammonium <sup>27,31</sup> or imidazolium cations, <sup>26</sup> among others. These structures are often monomeric, but linear polymers based on these interactions have also been studied in solution and the solid state. 32-36 We hypothesized that these principles could be applied to orient polyfunctional ion pairs as extended, ordered networks. Here, we report that C4Ps can bind dimethyl 1,4-diazabicyclo[2.2.2]octane (DABCO) dications, along with various polyfunctional carboxylate linkers to form crystalline framework assemblies, with ladder or layered two-dimensional (2D) topologies, all of which were characterized by single-crystal X-ray diffraction (SCXRD). We explore structural features that influence whether ladder or 2D supramolecular assemblies are formed. Some of these materials are sufficiently robust to withstand activation to permanently porous structures. Finally, the development of solid-state molecular arrays of spin-active building blocks is a current area of significant interest for quantum information science applications. 37,38 We demonstrate that C4P assemblies can be leveraged as a means to assemble spin-active building blocks into molecular arrays. Specifically, we demonstrate that tetrathifulvalene (TTF) tetracarboxylates, whose electronic excited states are of interest for quantum information science applications, can be ordered into solid-state arrays and characterized by electron paramagnetic resonance (EPR).

#### **RESULTS AND DISCUSSION**

Meso-octamethyl-calix[4]pyrrole (1), dimethyl 1,4-diazabicyclo[2.2.2]octane diiodide ( $2 \cdot 21^-$ ), and trimesic acid ( $3 \cdot 3H^+$ ) were dissolved in dimethyl sulfoxide, after which tetrabutylammonium hydroxide (3 equiv with respect to  $3 \cdot 3H^+$ ) was added. The preference for 1 to bind carboxylates and quaternary ammonium ions induced the exchange of the iodide counter ions of 2 with the carboxylates of 3, which resulted in the formation of monoclinic crystals (1:2:3) suitable for SCXRD. The crystal

m-wasielewski@northwestern.edu (M.R.W.), wdichtel@northwestern.edu (W.R.D.) https://doi.org/10.1016/j.chempr.2023.01.011

<sup>&</sup>lt;sup>1</sup>Department of Chemistry, Northwestern University, 2045 Sheridan Road, Evanston, IL 60208, USA

<sup>&</sup>lt;sup>2</sup>Lead contact

<sup>\*</sup>Correspondence:





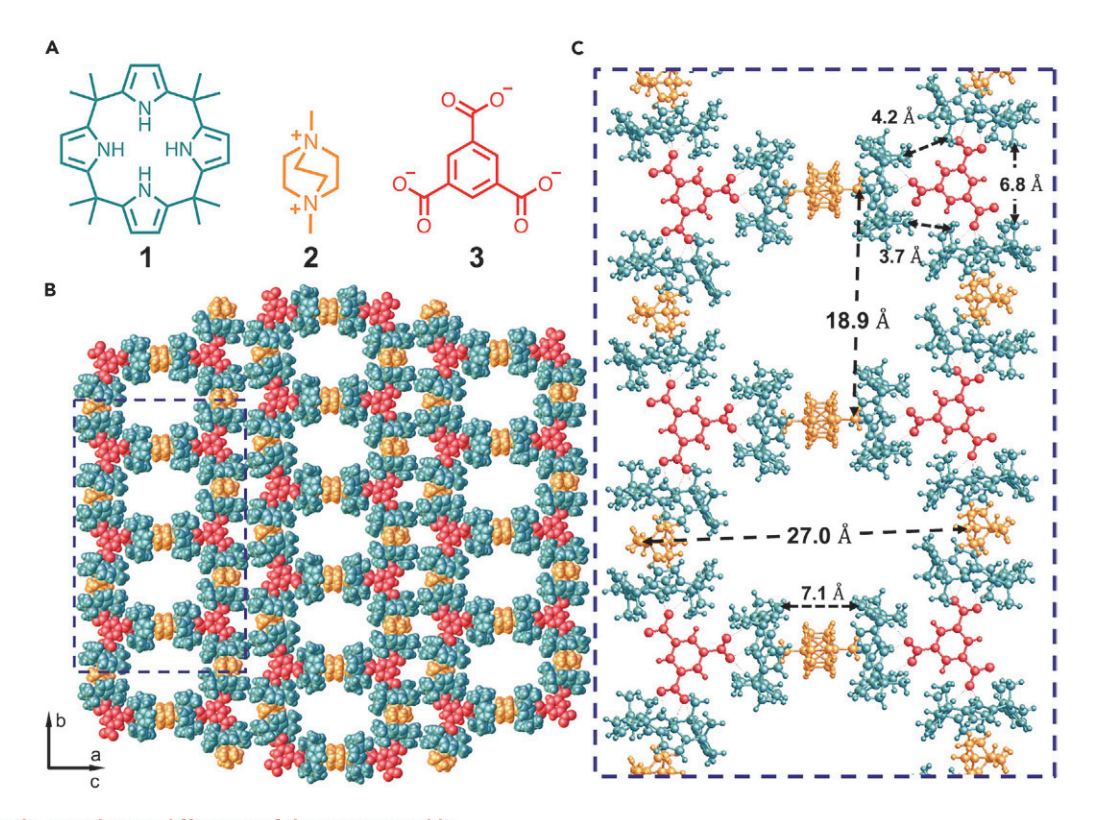


Figure 2. Single-crystal X-ray diffraction of the 1:2:3 assembly

(A) Building blocks used in the synthesis of supramolecular ladder assemblies.

(B) Single-crystal X-ray structure of supramolecular ladder assemblies composed of 1, 2, and 3. Solvent molecules have been removed for clarity. (C) Enlarged ball and stick structures that correspond to the dashed boxes present in (B), and 2 and one-third of the molecules of 1 bind the methyl groups of 2 in a colinear arrangement, with 7.1 Å spacing from one C4P to another. The other molecules of 1 bind 2 in a side-on fashion that enables the overall ladder polymer structure.

structure revealed that 1 binds 2 and 3 so as to form a supramolecular ladder polymer (Figures 2 and S1), and 1 binds the aryl carboxylates through multidentate NH···O hydrogen bonding interactions. Each 1,3,5-benzenetricarboxylate ion binds three C4Ps, which in turn also bind 2 within the electron-rich pocket at the opposite face of 1. This arrangement is favorable because of the complementary size of 2 and the C4P, which allows for close ion contacts with the anionic carboxylate guest 3.39 Because 2 is a dication, it can bind two different C4Ps, enabling the formation of extended structures when a polyfunctional carboxylate such as 3 is also employed. This binding arrangement typically occurs in a collinear fashion (closest  $d_{C...C}$  = 7.1 Å), with the methyl group of 2 occupying the electron-rich cavity of 1. However, this colinear arrangement is observed for only one C4P per 1,3,5-benzenetricarboxylate unit in the crystal (one-third of the C4Ps). The other two-thirds of the C4Ps bind 2 in an alternate, side-on geometry, which enables the C4Ps to adopt a non-linear arrangement. This geometry results in the closer spacing of the C4Ps (closest  $d_{C...C} = 4.0$  or 6.4 Å) and bowing of the carboxylate:1:2 geometry, which provides the ladder structure instead of the crystal tiling in two dimensions, and 1:2:3 ladders exhibit solvent-accessible, nanometer-scale pores with the longest dimensions of 2.70 nm by 1.89 nm (Figure 2C), which are uncommon in solid-state materials bound by Coulombic forces.

Based on the 1:2:3 structure, we hypothesized that porous 2D assemblies might be formed by varying the polyfunctional carboxylate structures to produce smaller voids,



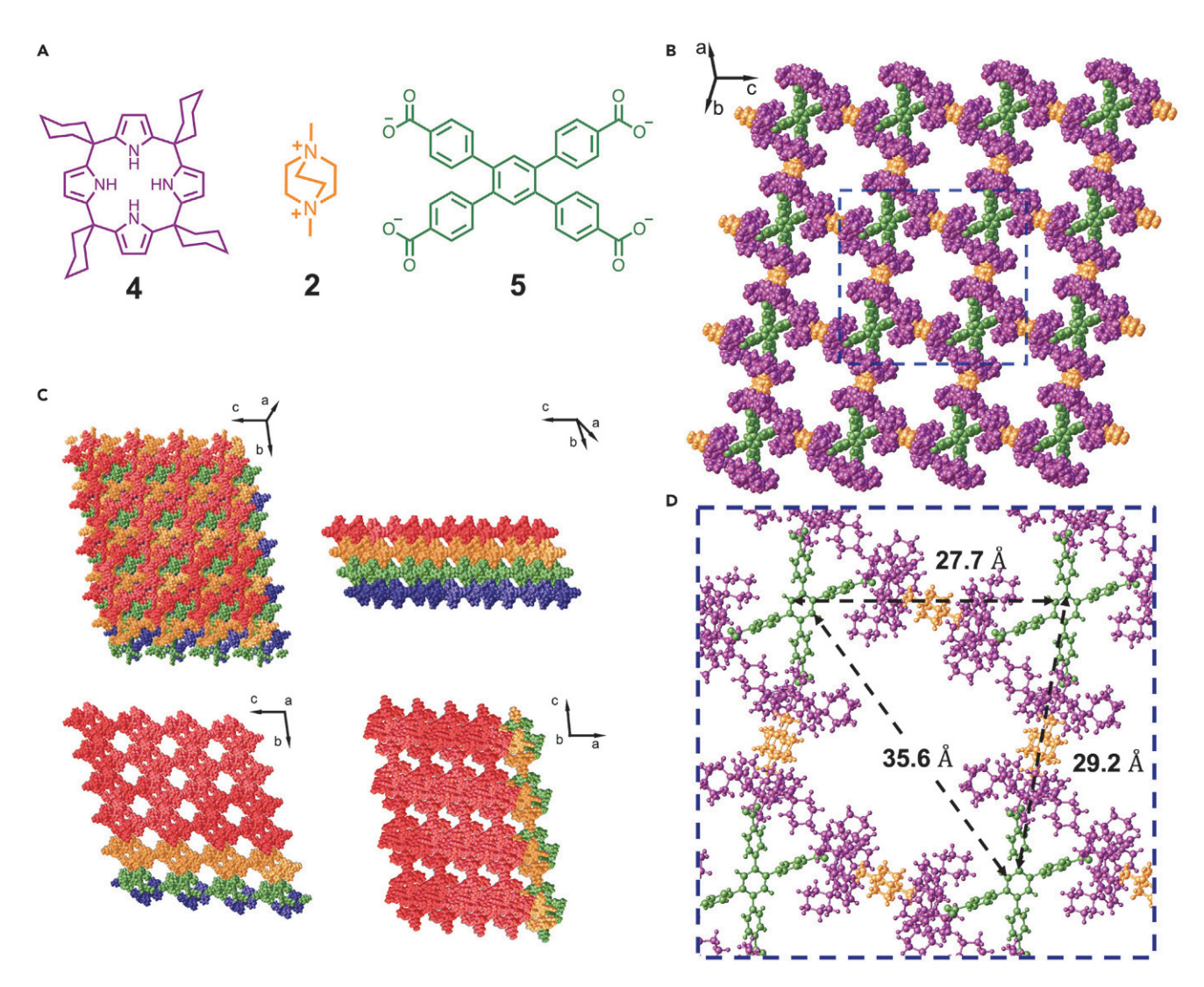


Figure 3. Single-crystal X-ray diffraction of the 4:2:5 assembly

(A) Building blocks used in the synthesis of two-dimensional supramolecular assemblies.

(B) Single-crystal X-ray structure of the two-dimensional supramolecular assembly composed of 4, 2, and 5. Solvent molecules have been removed for clarity.

(C) Single-crystal X-ray structures depicting the stacking of layers of the assembly. Different crystallographic orientations demonstrate an offset stacking of the supramolecular sheets as well as two-pore sizes.

(D) Enlarged ball and stick structure that corresponds to the dashed box present in (B). Atomic distances highlight the large void space present in the two-dimensional assembly with a width of 35.6 Å and a length of 41.0 Å at their widest points.

as well as by introducing larger groups on the periphery of the C4P macrocycle. We evaluated these design criteria using tetrakis(spirocyclohexane)calix[4]pyrrole (4) in place of 1 and 1,2,4,5-tetrakis(4-carboxyphenyl)benzene ( $5\cdot4H^+$ ) in place of 3 (Figure 3A). This assembly was synthesized in a similar manner to 1:2:3 in which 4,  $2\cdot2I^-$  and  $5\cdot4H^+$  were dissolved in dimethylformamide. After tetrabutylammonium methoxide (6 equiv with respect to  $5\cdot4H^+$  for optimal crystal quality), triclinic single crystals (4:2:5) formed, which were analyzed via SCXRD. Indeed, 4:2:5 forms 2D assemblies with large, solvent-accessible pores (Figure 3B). The pores have a triclinic-like topology and are 2.77 nm wide and 2.92 nm tall, with diagonal widths of 3.56 and 4.10 nm (Figure 3D). These dimensions are comparable with those of typical 2D COFs or MOFs. The 2D sheets of 4:2:5 stack in an offset manner, which occurs predominantly along the 001





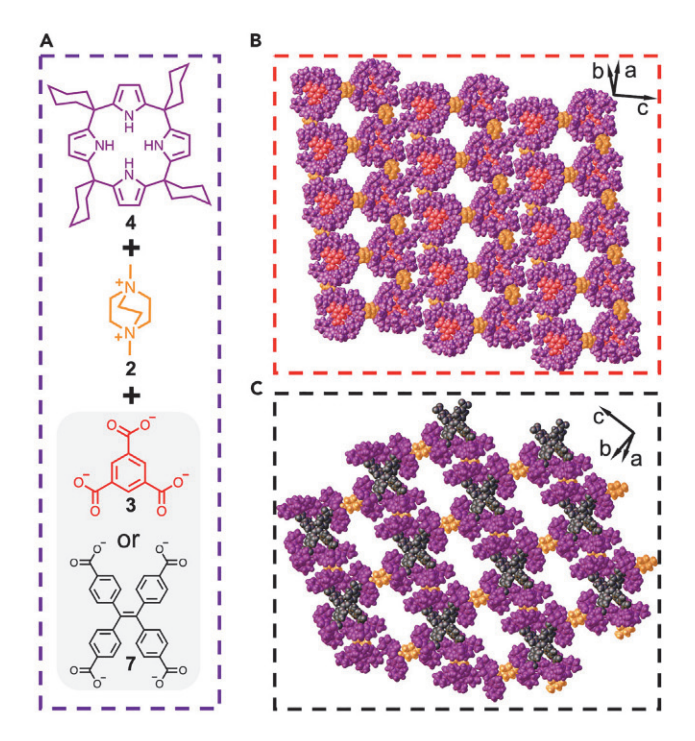


Figure 4. Single-crystal X-ray diffraction of assemblies that show the effects of varying the carboxylate linker symmetry

- (A) Building blocks used in the assemblies depicted in (B) and (C).
- (B) Single-crystal structure of ladder assemblies composed of 4, 2, and 3.
- (C) Single-crystal structure of two-dimensional assemblies composed of 4, 2, and 7. Coloring of
- (B) and (C) correlate to the different building blocks described in (A). Solvent molecules have been removed for clarity for both (B) and (C).

lattice plane with an offset of 12.5 Å (Figure 3C). Moreover, the offset stacking results in the presence of two-pore topologies within the bulk crystal. For example, the crystal has pore windows along its a axis and b axis that are ca. 17 and 13 Å wide, respectively. In addition to SCXRD studies, the solvent stability of the 4:2:5 assembly was also assessed. In situ powder X-ray diffraction (PXRD) of the 4:2:5 assembly established that these assemblies maintain their crystallinity in a number of solvents including ethanol (see below), hexanes, diethyl ether, dimethyl formamide, and acetonitrile (Figure S7).

The 1:2:3 ladder and 4:2:5 2D assemblies raised questions as to how the building block structure directs the formation of either ladders or 2D sheets. First, we studied how the polyfunctional carboxylate influenced the relative orientations of the larger C4P derivative 4 in the solid state. We combined 4 and  $2 \cdot 21^-$  with either  $3 \cdot 3H^+$ , or 1,1,2,2-tetra(4carboxyphenyl)ethylene (6·4H+) in dimethylformamide, followed by treatment with tetrabutylammonium methoxide (Figure 4A). Both mixtures formed single crystals of sufficient quality for SCXRD. The 4:2:3 assembly, forms supramolecular ladder-type structures (Figures 4B, S2, and S3), suggesting that the cyclohexyl groups on 4 alone do not ensure the formation of a 2D network. This assembly is similar to the 1:2:3 ladder in that two-thirds of its C4P units bind to that of trimesic acid in the non-colinear fashion associated with the ladder structures (see supplemental information for more details of the structure). When 4 is combined with 6, which has a similar  $D_{2h}$  symmetry as 5, we obtained another 2D assembly (Figures 4C and S4). This assembly shared similar characteristics as the 4:2:5 assembly, notably the formation of 2D sheets that stack in an offset fashion. Both the 4:2:3 and the 4:2:6 assemblies have large, triclinic voids: those



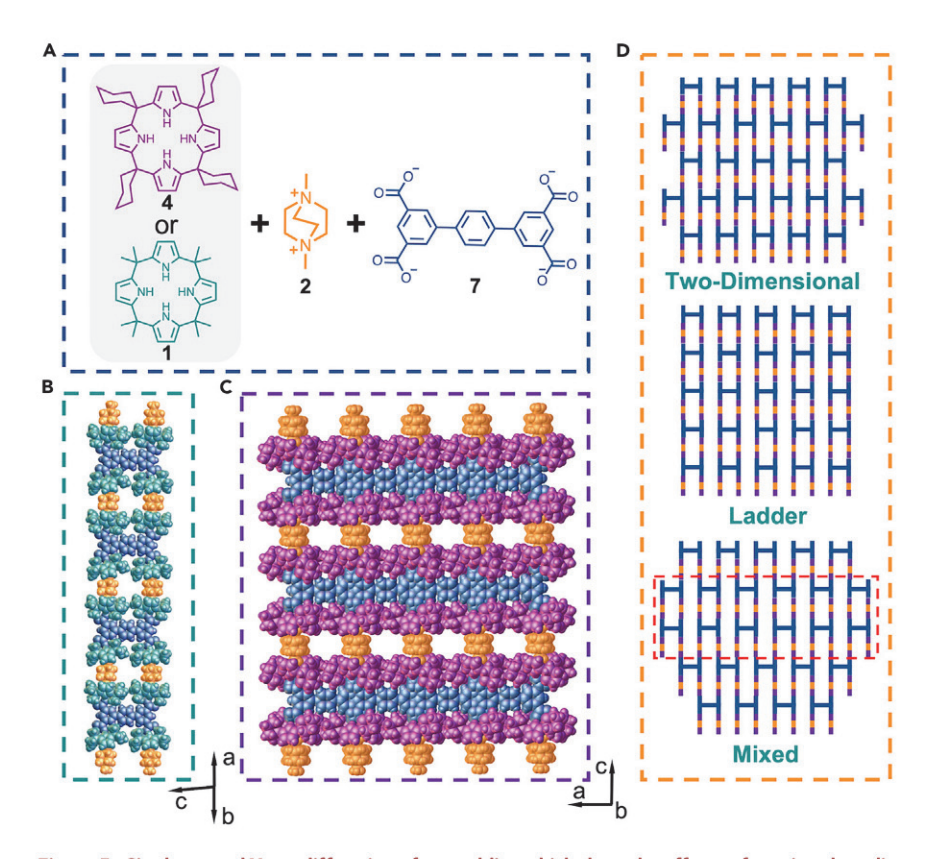


Figure 5. Single-crystal X-ray diffraction of assemblies which show the effects of varying the calix [4]pyrrole identity

- (A) Building blocks used in the assemblies depicted in (B) and (C).
- (B) Single-crystal structure of ladder assemblies composed of 1, 2, and 7.
- (C) Single-crystal structure of two-dimensional assemblies composed of 4, 2, and 7. Coloring of
- (B) and (C) correlate to the different building blocks described in (A). Solvent molecules have been removed for clarity for both (B) and (C).
- (D) Cartoon representation of possible assembly types for the 4:2:7 assembly. The ladder domain of the mixed assembly type is highlighted in red.

of the 4:2:3 assembly are 2.65 nm wide and 1.92 nm tall, whereas those of the 4:2:6 assembly are 2.92 nm wide and 2.42 nm tall.

We also investigated the role of the C4P macrocycle structures in selecting for ladders or 2D networks using another monomer with D<sub>2h</sub> symmetry, p-terphenyl-3.3'', 5.5''-tetracarboxylic acid  $(7.4H^+)$ , along with  $2.2I^-$  and either 1 or 4 (Figure 5A). C4P 1 provided a 1:2:7 ladder assembly with rectangular voids that were 1.87 nm tall and 1.09 nm wide (Figures 5B and S5). Unlike the previously described ladder assemblies, the 1:2:7 ladder can accommodate all of the C4Ps having colinear interactions with 2. When 4 was used in place of 1, the high symmetry of the system resulted in a crystal with fractional occupancies of 7 in which two different assembly types are possible in the crystal network (Figure 5D). This fractional occupancy is apparent in the crystal structure where 7 shows no clear directionality within the network (Figures 5C and S6). This unique case allows the 4:2:7 assembly to be simultaneously assembled in two dimensions or as a ladder assembly. We attribute this effect to the high symmetry of the unit cell as well as 7 having the ideal spacing to allow for either assembly type. Overall, these structural observations indicate that both the polyfunctional carboxylate structure and the C4P peripheral groups affect the assembly. Notably, the 1:2:7 ladder has a non-centrosymmetric P2<sub>1</sub> space group, which is





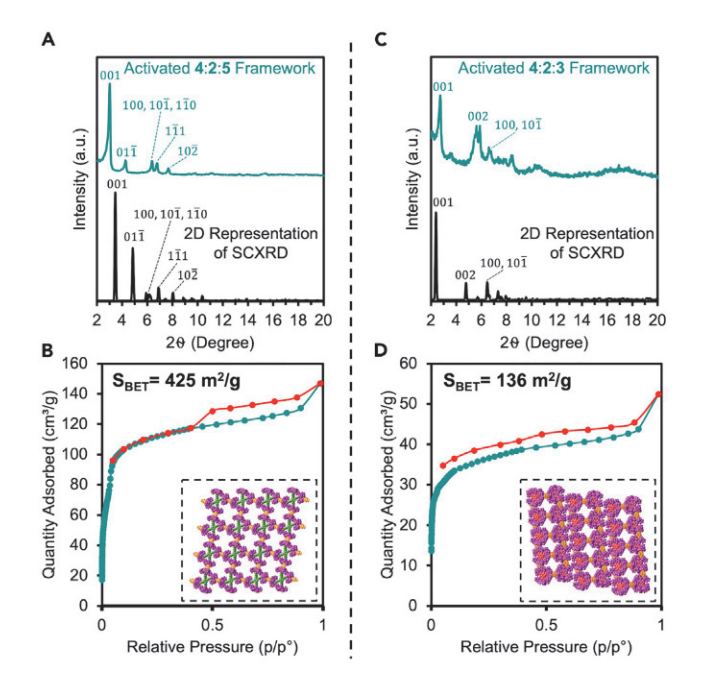


Figure 6. Powder X-ray diffraction and porosimetry measurements of activated 4:2:5 and 4:2:3 assemblies

(A) Powder X-ray diffraction of two-dimensional assemblies composed of 4, 2, and 5 after activation as well as a two-dimensional representation of experimental single-crystal X-ray diffraction data. (B)  $N_2$  adsorption and desorption isotherm of the 4:2:5 assembly. Inset is of the 4:2:5 single-crystal X-ray structure.

(C) Powder X-ray diffraction of ladder assemblies composed of 4, 2, and 3 after activation as well as a two-dimensional representation of experimental single-crystal X-ray diffraction data.

(D)  $N_2$  adsorption and desorption isotherm of the 4:2:3 assembly. Inset is of the 4:2:3 single-crystal X-ray structure.

relatively rare, particularly for a crystal composed of achiral components. Crystalline materials with non-centrosymmetric space groups are of interest for their non-linear optical and ferroelectric properties, <sup>40–42</sup> such that exploring the modularity of these ladder structures is an important next step.

We next explored methods to remove the solvent while preserving the long-range order of the 4:2:5 2D assembly and the 4:2:3 ladder polymer. The 4:2:5 and 4:2:3 crystals underwent solvent exchange for 48 h in either ethanol or acetone, respectively, followed by supercritical CO2 activation. Thermogravimetric analysis was performed on both assemblies and showed the first significant mass loss at ca. 220°C, which suggests good thermal stability and that little to no solvent is retained following activation (Figure S15). PXRD of the activated 4:2:5 crystals revealed a high degree of crystallinity with a diffraction pattern that matches a pattern derived from the single-crystal structure (Figure 6A). Variations in the experimental PXRD are attributed to small shifts of the 001 and  $01\overline{1}$  peaks due to a slight expansion of the unit cell after activation. These shifts are common in porous organic crystals due to their flexible nature. 43 The PXRD of the 4:2:3 assembly after activation also maintains a good degree of crystallinity that matches the 2D powder pattern derived from the experimental single-crystal X-ray diffraction data (Figure 6C). However, instead of an expansion of the unit cell, the 4:2:3 assembly exhibited a shift of both the 001 and 002 peaks toward smaller d-spacing. N<sub>2</sub> adsorption and desorption isotherms were performed on 4:2:5 and 4:2:3, resulting in surface areas of 425 and 136 m<sup>2</sup>/g, respectively





(Figures 6B and 6D). Pore distribution analysis of the 4:2:5 assembly displayed two well-defined pore sizes of 17.0 and 12.5 Å (Figure S13). This analysis is consistent with the pore sizes observed in the bulk crystal structure. In the case of the 4:2:3 assembly, pore size distribution analysis was also consistent with the solid-state structure, although hysteresis observed in the low-pressure region of the isotherm makes this conclusion less reliable (Figure S14). These findings demonstrate that the C4P assemblies are sufficiently robust to withstand solvent removal without significant structural changes.

Using these porous and relatively modular assemblies to organize arrays of electronically interesting components for quantum information science applications is desirable as a means to control their relative distances and orientations and feature high materials quality, low potential for charge mobility, tunable spacing of arrayed building blocks, solvent-accessible pores, and are composed of light elements with low nuclear spin. <sup>37,38</sup> This platform could provide a new strategy in the pursuit of molecularly precise solid-state spin arrays whose properties can be precisely characterized and rationally tuned. As a proof of concept, we incorporated tetrathiafulvalene-tetrabenzoate ( $8.4H^+$ ) because of its  $D_{2h}$  symmetry, synthetic availability, and ability to form triplet states when photoexcited. 44 A 2D supramolecular polymer network was obtained from a mixture of  $4, 2 \cdot 2I^-$ , and  $8 \cdot 4H^+$ , which was treated with tetrabutylammonium methoxide in dimethylformamide (Figure 7A). Large triclinic single crystals were obtained and characterized via SCXRD (Figure 7B). The 4:2:8 assembly contained solvent-accessible voids with a triclinic-like topology. The dimensions of these pores were the largest of any C4P assembly we have obtained to date, with voids of 3.14 nm wide and 3.20 nm tall (Figure 7D), and diagonal widths of 3.70 and length of 4.55 nm, respectively. Additionally, similar to the 4:2:5 assembly, the 2D sheets of the 4:2:8 assembly stack in an offset manner—this offset occurs predominantly along the  $01\overline{3}$  lattice plane with a distance of 13.8 Å (Figure 7C).

Following full structural characterization of the 4:2:8 assembly, EPR spectroscopy was performed on the 4:2:8 assembly as well as on the tetrathiafulvalene monomer (8) in both its protonated and deprotonated forms. Transient EPR (TREPR) experiments were performed at 85 K with the crystals suspended in butyronitrile and the monomers dissolved in ethanol. All compounds were photoexcited with a 520 nm, 7 ns laser pulse at the shoulder of their lowest energy visible absorption band (Figure \$16). The triplet TREPR spectrum at 140 ns after the laser pulse was fit using EasySpin (Figures 8, \$18, and \$19). The fits provide the zero-field splitting values D and E of the triplet state (Figure S20). In addition, at the low field end of the 4:2:8 assembly, the TREPR spectrum shows a sharp emissive feature, which is the double quantum transition of the triplet state. The presence of the double quantum transition confirms the assignment of the observed transient species to that of a triplet, which is consistent with the spectral simulations. The zero-field splitting values obtained from the simulation are |D| = 5,197 MHz and |E| = 695 MHz, which are in the range of those observed for other tetrathiafulvalene derivatives.<sup>44</sup> Comparing the zero-field splitting constants of the 4:2:8 assembly with those of the monomers shows that D is smaller in the monomers by about 1 GHz, which suggests that the TTF triplet state in the assembly is more localized. By applying a simple point dipole approximation, 45 the average distance between electron spins in the triplet state of the 4:2:8 assembly is about 0.2 Å smaller than that in the monomers. The zero-field splitting parameter, E, gives information on the symmetry of the localized triplet state. The ratio E/D is maximally 1/3 and would indicate a rhombic or asymmetric distribution of triplet electron density. Smaller values of E/D indicate a more axial or symmetric distribution.<sup>46</sup> Here, E/D is 0.13 for the crystals, 0.17 for





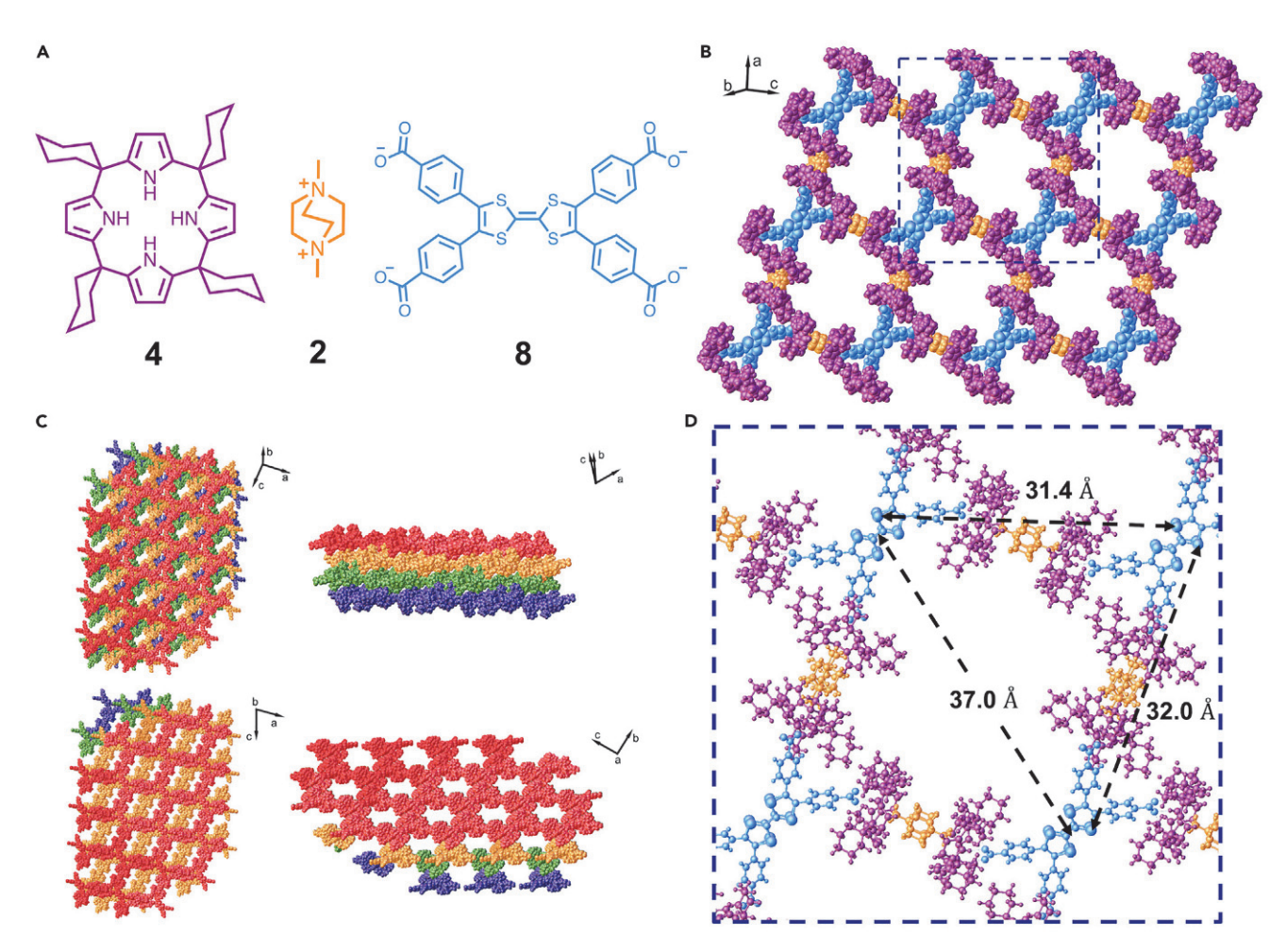


Figure 7. Single-crystal X-ray diffraction of the 4:2:8 assembly

(A) Reactants used in the synthesis of a two-dimensional tetrathiafulvalene supramolecular assembly. (B) Single-crystal structure of two-dimensional supramolecular composed of 4, 2, and 8. Solvent molecules have been removed for clarity.

(C) Single-crystal structures viewed from different crystallographic orientations illustrate how the two-dimensional sheets stack with respect to each other within the crystal and the resulting pore topologies.

(D) Enlarged ball and stick structure that corresponds to the dashed box present in (B). Atomic distances highlight the large void structures present in the two-dimensional assembly with 37.0 and 45.5 Å of void space at the widest points.

the protonated monomer, and 0.15 for the deprotonated monomer. Therefore, the electron distribution for all three species in this study is approximately the same and is more axial than rhombic. The widths of these triplet spectra make them promising candidates for the manipulation of individual spin states for various quantum information applications. As has been seen with  $C_{60}$  derivatives,  $^{47}$  the triplet spin states can be selectively manipulated and addressed using pulse-EPR spectroscopy. The triplet state spectrum of C<sub>60</sub> derivatives is about 100-150 mT wide, which allows for different regions of the triplet spectrum to be addressed. The 300–400 mT wide triplet signals seen in this study (excluding the double quantum transition) provides even more flexibility for specific addressability with spin manipulations (Figure 8). With the modular synthetic flexibility of C4P assemblies, other spectrally addressable systems might be accessed. Such systems could be triplet states with tuned zero-field splitting parameters, radical pairs, or other multi-spin systems that can be manipulated with pulse-EPR spectroscopy. Additionally, the phosphorescence emission of molecular triplet states enables more sensitive detection methods such as optically detected magnetic resonance (ODMR).



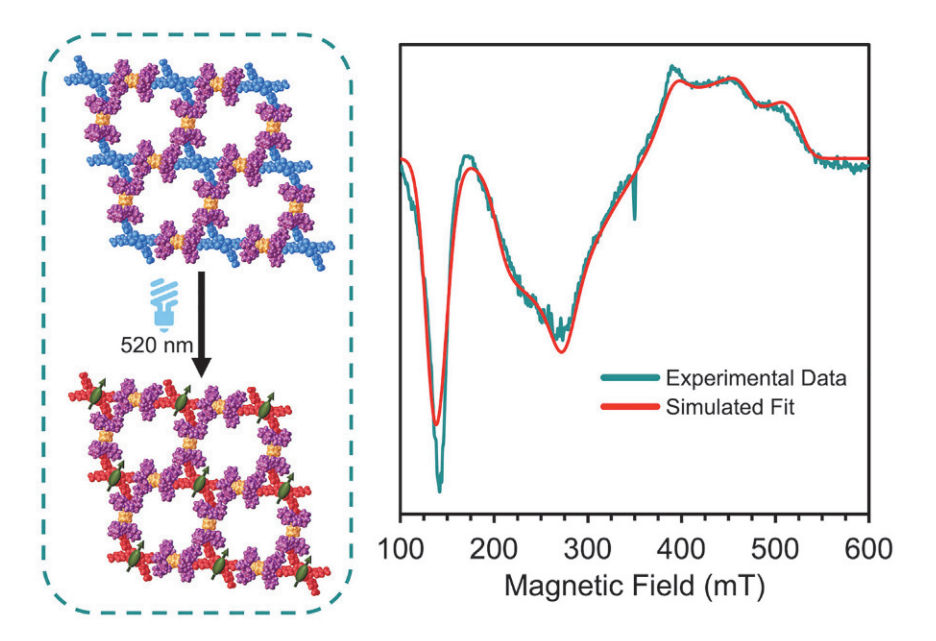


**Figure 8. Transient electron paramagnetic resonance spectroscopy of the 4:2:8 assembly** TREPR spectrum of the tetrathiafulvalene assembly at 140 ns after a 520 nm, 7 ns laser pulse. The blue trace is the experimental data and the red trace is the fit.

#### Conclusions

C4Ps in the presence of 2 and a multifunctional carboxylate form crystalline, porous assemblies based on ion-pair recognition. Additionally, these assemblies were shown to be modular with the carboxylate linker and C4P macrocycle being easily varied. Although all examples in this work use 2 as the multifunctional cation, it is likely that other cations capable of binding to C4Ps can be used. SCXRD revealed that this high degree of modularity could be leveraged to tune the assembly structure to form either ladder assemblies or 2D assemblies, which depended both on the carboxylate structure and the steric bulk on the periphery of the C4P. The steric bulk of 4 combined with the closely spaced carboxylates of the D<sub>2h</sub> monomers enforces the head-on carboxylate-C4P interactions to favor the formation of 2D assemblies. Moreover, PXRD and gas isotherm measurements demonstrated that it is possible to remove the solvent from these assemblies and maintain their porous, high-surface-area structures. Finally, spin-active tetrathiafulvalene monomers were incorporated into 2D assemblies that were characterized by single-crystal X-ray diffraction. These assemblies were photoexcited at 520 nm to form spinactive, TTF-based triplet states that were characterized with TREPR spectroscopy. These results demonstrate that this new ion-pair assembly strategy can provide molecular arrays with interesting magnetic and electronic properties as large single crystals that contain only light elements. In the future, it should be possible to vary the composition of these assemblies and the relative distances and orientations of their active elements for emergent functions such as quantum bit arrays. Overall, these assemblies are highly modular, porous, composed of organic building blocks, and easily form large single crystals. These assemblies might also leverage other known C4P derivatives, as well as monomers containing other functional groups that C4Ps bind. 23,24 These materials occupy a unique chemical space inaccessible to other conventional framework technologies, which makes C4P frameworks a particularly appealing platform for studying their unique properties, especially in relation to quantum information processing. Future efforts are focused on leveraging new types of building blocks for the incorporation of new spin-active





building blocks and studying the manipulation of these spins within the C4P network.

#### **EXPERIMENTAL PROCEDURES**

#### Resource availability

#### Lead contact

Further information and requests for resources should be directed to and will be fulfilled, where possible, by the lead contact, William R. Dichtel (wdichtel@northwestern.edu).

#### Materials availability

The experimental dataset and materials generated are available from the lead contact upon reasonable request.

#### Data and code availability

CCDC 2203882, 2203883, 2203884, 2203885, 2203886, 2203887, and 2204202 contains the supplementary crystallographic data for this paper. These data can be obtained free of charge via <a href="www.ccdc.cam.ac.uk/data\_request/cif">www.ccdc.cam.ac.uk/data\_request/cif</a>, or by emailing data\_request@ccdc.cam.ac.uk, or by contacting The Cambridge Crystallographic Data Centre, 12 Union Road, Cambridge CB2 1EZ, UK; fax: +44 1223 336033.

#### SUPPLEMENTAL INFORMATION

Supplemental information can be found online at https://doi.org/10.1016/j.chempr. 2023.01.011.

#### **ACKNOWLEDGMENTS**

This work was supported by the National Science Foundation under award DMR-2003739 (M.R.W.). L.P.S. and Z.H. were supported by NSF Graduate Research fellowships under grant DGE-1842165. This work made use of the Integrated Molecular Structure Education and Research Center (IMSERC) at Northwestern University, which has received support from the NSF (CHE-1048773), the Soft and Hybrid Nanotechnology Experimental (SHyNE) Resource (NSF; NNCI-1542205), the State of Illinois, and the International Institute for Nanotechnology(IIN).

#### **AUTHOR CONTRIBUTIONS**

Conceptualization, L.P.S. and W.R.D.; investigation, L.P.S., C.L.S., L. B., C. M., C.P., X.A.-E., and J.L.S.; formal analysis, L.P.S., C.L.S., and L.B.; writing – original draft, L.P.S., M.R.W., and W.R.D.; writing – review and editing, all authors; supervision, M.R.W. and W.R.D.; funding acquisition, L.P.S., L. B., C. M., C.P., X.A.-E., J.L.S., M.R.W., and W.R.D.

#### **DECLARATION OF INTERESTS**

The authors declare no conflicts of interest.

#### **INCLUSION AND DIVERSITY**

We support inclusive, diverse, and equitable conduct of research.

Received: August 30, 2022 Revised: December 19, 2022 Accepted: January 18, 2023 Published: February 13, 2023





#### **REFERENCES**

- Savyasachi, A.J., Kotova, O., Shanmugaraju, S., Bradberry, S.J., Ó'Máille, G.M., and Gunnlaugsson, T. (2017). Supramolecular chemistry: a toolkit for soft functional materials and organic particles. Chem 3, 764–811. https://doi.org/10.1016/j.chempr.2017.10.006.
- Yang, L., Tan, X., Wang, Z., and Zhang, X. (2015). Supramolecular polymers: historical development, preparation, characterization, and functions. Chem. Rev. 115, 7196–7239. https://doi.org/10.1021/cr500633b.
- Hu, H., Gopinadhan, M., and Osuji, C.O. (2014). Directed self-assembly of block copolymers: a tutorial review of strategies for enabling nanotechnology with soft matter. Soft Matter 10, 3867–3889. https://doi.org/10.1039/ C35M52607K.
- Karayianni, M., and Pispas, S. (2021). Block copolymer solution self-assembly: recent advances, emerging trends, and applications. J. Polym. Sci. 59, 1874–1898. https://doi.org/ 10.1002/pol.20210430.
- Zhu, J., Avakyan, N., Kakkis, A., Hoffnagle, A.M., Han, K., Li, Y., Zhang, Z., Choi, T.S., Na, Y., Yu, C.-J., and Tezcan, F.A. (2021). Protein assembly by design. Chem. Rev. 121, 13701– 13796. https://doi.org/10.1021/acs.chemrev. 1c00308.
- 6. Luo, Q., Hou, C., Bai, Y., Wang, R., and Liu, J. (2016). Protein assembly: versatile approaches to construct highly ordered nanostructures. Chem. Rev. 116, 13571–13632. https://doi.org/10.1021/acs.chemrev.6b00228.
- Grzelczak, M., Vermant, J., Furst, E.M., and Liz-Marzán, L.M. (2010). Directed self-assembly of nanoparticles. ACS Nano 4, 3591–3605. https://doi.org/10.1021/nn100869j.
- Boles, M.A., Engel, M., and Talapin, D.V. (2016). Self-assembly of colloidal nanocrystals: from intricate structures to functional materials. Chem. Rev. 116, 11220–11289. https://doi.org/ 10.1021/acs.chemrev.6b00196.
- Aida, T., Meijer, E.W., and Stupp, S.I. (2012). Functional supramolecular polymers. Science 335, 813–817. https://doi.org/10.1126/science. 1205962.
- Stein, A., Wright, G., Yager, K.G., Doerk, G.S., and Black, C.T. (2016). Selective directed selfassembly of coexisting morphologies using block copolymer blends. Nat. Commun. 7, 12366. https://doi.org/10.1038/ncomms12366.
- Terzic, I., Meereboer, N.L., Acuautla, M., Portale, G., and Loos, K. (2019). Electroactive materials with tunable response based on block copolymer self-assembly. Nat. Commun. 10, 601. https://doi.org/10.1038/s41467-019-08436-2.
- Wang, Z., Chan, C.L.C., Zhao, T.H., Parker, R.M., and Vignolini, S. (2021). Recent advances in block copolymer self-assembly for the fabrication of photonic films and pigments. Adv. Optical Mater. 9, 2100519. https://doi. org/10.1002/adom.202100519.
- Huang, C., Chen, X., Xue, Z., and Wang, T. (2020). Effect of structure: a new insight into nanoparticle assemblies from inanimate to

- animate. Sci. Adv. 6, eaba1321. https://doi.org/ 10.1126/sciadv.aba1321.
- Grzelczak, M., Liz-Marzán, L.M., and Klajn, R. (2019). Stimuli-responsive self-assembly of nanoparticles. Chem. Soc. Rev. 48, 1342–1361. https://doi.org/10.1039/C8CS00787J.
- Furukawa, H., Cordova, K.E., O'Keeffe, M., and Yaghi, O.M. (2013). The chemistry and applications of metal-organic frameworks. Science 341, 1230444. https://doi.org/10.1126/ science.1230444.
- Bisbey, R.P., and Dichtel, W.R. (2017). Covalent organic frameworks as a platform for multidimensional polymerization. ACS Cent. Sci. 3, 533–543. https://doi.org/10.1021/ acscentsci.7b00127.
- Evans, A.M., Strauss, M.J., Corcos, A.R., Hirani, Z., Ji, W., Hamachi, L.S., Aguilar-Enriquez, X., Chavez, A.D., Smith, B.J., and Dichtel, W.R. (2022). Two-dimensional polymers and polymerizations. Chem. Rev. 122, 442–564. https://doi.org/10.1021/acs.chemrev.0c01184.
- Li, P., Ryder, M.R., and Stoddart, J.F. (2020). Hydrogen-bonded organic frameworks: A rising class of porous molecular materials. Acc. Mater. Res. 1, 77–87. https://doi.org/10.1021/ accountsmr.0c00019.
- Wang, B., Lin, R.B., Zhang, Z., Xiang, S., and Chen, B. (2020). Hydrogen-bonded organic frameworks as a tunable platform for functional materials. J. Am. Chem. Soc. 142, 14399–14416. https://doi.org/10.1021/jacs.0c06473.
- He, Q., Vargas-Zúñiga, G.I., Kim, S.H., Kim, S.K., and Sessler, J.L. (2019). Macrocycles as ion pair receptors. Chem. Rev. 119, 9753–9835. https://doi.org/10.1021/acs.chemrev.8b00734.
- Kim, S.K., and Sessler, J.L. (2010). Ion pair receptors. Chem. Soc. Rev. 39, 3784–3809. https://doi.org/10.1039/C002694H.
- Gale, P.A., Sessler, J.L., Král, V., and Lynch, V. (1996). Calix[4]pyrroles: old yet new anion-binding agents. J. Am. Chem. Soc. 118, 5140–5141. https://doi.org/10.1021/ja960307r.
- Kim, S.K., and Sessler, J.L. (2014). Calix[4] pyrrole-based ion pair receptors. Acc. Chem. Res. 47, 2525–2536. https://doi.org/10.1021/ ar500157a.
- Kim, D.S., and Sessler, J.L. (2015). Calix[4] pyrroles: versatile molecular containers with ion transport, recognition, and molecular switching functions. Chem. Soc. Rev. 44, 532–546. https://doi.org/10.1039/C4CS00157E.
- Park, I.-W., Yoo, J., Kim, B., Adhikari, S., Kim, S.K., Yeon, Y., Haynes, C.J.E., Sutton, J.L., Tong, C.C., Lynch, V.M., et al. (2012).
  Oligoether-strapped calix[4]pyrrole: an ion-pair receptor displaying cation-dependent chloride anion transport. Chemistry 18, 2514–2523. https://doi.org/10.1002/chem. 201103239.
- Custelcean, R., Delmau, L.H., Moyer, B.A., Sessler, J.L., Cho, W.-S., Gross, D., Bates, G.W., Brooks, S.J., Light, M.E., and Gale, P.A. (2005). Calix[4]pyrrole: an old yet new ion-pair receptor. Angew. Chem. Int. Ed. Engl. 44,

- 2537–2542. https://doi.org/10.1002/anie. 200462945.
- Adriaenssens, L., Estarellas, C., Jentzsch, A.V., Belmonte, M.M., Matile, S., and Ballester, P. (2013). Quantification of nitrate—π interactions and selective transport of nitrate using calix[4] pyrroles with two aromatic walls. J. Am. Chem. Soc. 135, 8324–8330. https://doi.org/10.1021/ ja4021793.
- Hirao, T., Kim, D.S., Chi, X., Lynch, V.M., Ohara, K., Park, J.S., Yamaguchi, K., and Sessler, J.L. (2018). Control over multiple molecular states with directional changes driven by molecular recognition. Nat. Commun. 9, 823. https://doi. org/10.1038/s41467-018-03220-0.
- Sokkalingam, P., Yoo, J., Hwang, H., Lee, P.H., Jung, Y.M., and Lee, C.-H. (2011). Salt (LiF) regulated fluorescence switching. Eur. J. Org. Chem. 2011, 2911–2915. https://doi.org/10. 1002/ejoc.201100359.
- Verdejo, B., Gil-Ramírez, G., and Ballester, P. (2009). Molecular recognition of pyridine N-oxides in water using calix[4]pyrrole receptors. J. Am. Chem. Soc. 131, 3178–3179. https://doi.org/10.1021/ja900151u.
- Sessler, J.L., Gross, D.E., Cho, W.S., Lynch, V.M., Schmidtchen, F.P., Bates, G.W., Light, M.E., and Gale, P.A. (2006). Calix[4]pyrrole as a chloride anion receptor: solvent and countercation effects. J. Am. Chem. Soc. 128, 12281–12288. https://doi.org/10.1021/ ia064012h.
- Yuvayapan, S., and Aydogan, A. (2019). Supramolecular calix[4]pyrrole polymers from a complementary pair of homoditopic host– guest molecules. Chem. Commun. (Camb) 55, 8800–8803. https://doi.org/10.1039/ C9CC02806D.
- Budak, A., and Aydogan, A. (2021). A calix[4] pyrrole-based linear supramolecular polymer constructed by orthogonal self-assembly. Chem. Commun. (Camb) 57, 4186–4189. https://doi.org/10.1039/D1CC01003D.
- 34. Park, J.S., Yoon, K.Y., Kim, D.S., Lynch, V.M., Bielawski, C.W., Johnston, K.P., and Sessler, J.L. (2011). Chemoresponsive alternating supramolecular copolymers created from heterocomplementary calix[4]pyrroles. Proc. Natl. Acad. Sci. USA 108, 20913–20917. https:// doi.org/10.1073/pnas.1115356108.
- Ji, X., Chi, X., Ahmed, M., Long, L., and Sessler, J.L. (2019). Soft materials constructed using calix[4]pyrrole- and "Texas-sized" box-based anion receptors. Acc. Chem. Res. 52, 1915– 1927. https://doi.org/10.1021/acs.accounts. 9b00187.
- Kim, D.S., Chang, J., Leem, S., Park, J.S., Thordarson, P., and Sessler, J.L. (2015). Redoxand pH-responsive orthogonal supramolecular self-assembly: an ensemble displaying molecular switching characteristics. J. Am. Chem. Soc. 137, 16038–16042. https://doi.org/ 10.1021/jacs.5b06524.
- Graham, M.J., Zadrozny, J.M., Fataftah, M.S., and Freedman, D.E. (2017). Forging solid-state Qubit design principles in a molecular furnace. Chem. Mater. 29, 1885–1897. https://doi.org/ 10.1021/acs.chemmater.6b05433.





- Wasielewski, M.R., Forbes, M.D.E., Frank, N.L., Kowalski, K., Scholes, G.D., Yuen-Zhou, J., Baldo, M.A., Freedman, D.E., Goldsmith, R.H., Goodson, T., et al. (2020). Exploiting chemistry and molecular systems for quantum information science. Nat. Rev. Chem. 4, 490–504. https://doi.org/10.1038/s41570-020-0200-5.
- Gross, D.E., Schmidtchen, F.P., Antonius, W., Gale, P.A., Lynch, V.M., and Sessler, J.L. (2008). Cooperative binding of calix[4]pyrrole-anion complexes and alkylammonium cations in halogenated solvents. Chemistry 14, 7822– 7827. https://doi.org/10.1002/chem. 200800899.
- Tayi, A.S., Kaeser, A., Matsumoto, M., Aida, T., and Stupp, S.I. (2015). Supramolecular ferroelectrics. Nat. Chem. 7, 281–294. https:// doi.org/10.1038/nchem.2206.

- Ok, K.M. (2016). Toward the rational design of novel noncentrosymmetric materials: factors influencing the framework structures. Acc. Chem. Res. 49, 2774–2785. https://doi.org/10. 1021/acs.accounts.6b00452.
- 42. Li, P.F., Liao, W.Q., Tang, Y.Y., Qiao, W., Zhao, D., Ai, Y., Yao, Y.F., and Xiong, R.G. (2019). Organic enantiomeric high-Tc ferroelectrics. Proc. Natl. Acad. Sci. USA 116, 5878–5885. https://doi.org/10.1073/pnas.1817866116.
- Lin, R.-B., and Chen, B. (2022). Hydrogenbonded organic frameworks: chemistry and functions. Chem 8, 2114–2135. https://doi.org/ 10.1016/j.chempr.2022.06.015.
- 44. Furukawa, K., Sugishima, Y., Fujiwara, H., and Nakamura, T. (2011). Photoinduced triplet states of photoconductive TTF derivatives

- including a fluorescent group. Chem. Lett. 40, 292–294. https://doi.org/10.1246/cl.2011.292.
- van der Waals, J.H. (2001). EPR of photoexcited triplet states: a personal account. Appl. Magn. Reson. 20, 545–561. https://doi.org/10. 1007/BF03162337.
- Weil, J.A., and Bolton, J.R. (2007). Electron Paramagnetic Resonance Elementary Theory and Practical Applications, Second Edition (John Wiley & Sons, Ltd). https://doi.org/10. 1002/04/70084987.
- Wang, Y.-X., Liu, Z., Fang, Y.-H., Zhou, S., Jiang, S.-D., and Gao, S. (2021). Coherent manipulation and quantum phase interference in a fullerene-based electron triplet molecular qutrit. npj Quantum Inf. 7, 1–8. https://doi.org/ 10.1038/s41534-021-00362-w.